Silylamide Complexes

Deutsche Ausgabe: DOI: 10.1002/ange.201505518
Internationale Ausgabe: DOI: 10.1002/anie.201505518

The Instability of $Ni\{N(SiMe_3)_2\}_2$: A Fifty Year Old Transition Metal Silylamide Mystery

Michelle Faust, Aimee M. Bryan, Akseli Mansikkamäki, Petra Vasko, Marilyn M. Olmstead, Heikki M. Tuononen, Fernande Grandjean, Gary J. Long, and Philip P. Power**

In memory of Gregory L. Hillhouse

Abstract: *The characterization of the unstable Ni^{II} bis(silylamide) $Ni\{N(SiMe_3)_2\}_2$ (**1**), its THF complex $Ni\{N(SiMe_3)_2\}_2$(THF) (**2**), and the stable bis(pyridine) derivative trans-$Ni\{N(SiMe_3)_2\}_2(py)_2$ (**3**), is described. Both **1** and **2** decompose at ca. 25 °C to a tetrameric Ni^{I} species, $[Ni\{N(SiMe_3)_2\}]_4$ (**4**), also obtainable from $LiN(SiMe_3)_2$ and $NiCl_2$(DME). Experimental and computational data indicate that the instability of **1** is likely due to ease of reduction of Ni^{II} to Ni^{I} and the stabilization of **4** through dispersion forces.*

In the early 1960s, Bürger and Wannagat reported that the bis(trimethylsilyl)amido ligand -$N(SiMe_3)_2$ stabilized the first 2- and 3-coordinate, open-shell transition-metal complexes.[1,2] These included the M^{II} species $Mn\{N(SiMe_3)_2\}_2$,[2] $Co\{N(SiMe_3)_2\}_2$,[1] and $Ni\{N(SiMe_3)_2\}_2$.[2] The corresponding Fe^{II} derivative, $Fe\{N(SiMe_3)_2\}_2$, was described in 1988.[3] Uniquely, the Ni^{II} amide was reported to be unstable, decomposing to a black solid at room temperature.[2] The Mn, Fe, and Co silylamides are thermally stable and have proven to be valuable synthons in diverse applications,[4–13] but the unstable nature of $Ni\{N(SiMe_3)_2\}_2$ has hindered its further use. Its instability is especially striking because several other stable, homoleptic Ni^{II} amides are known. These include $\{Ni(NPh_2)_2\}_2$,[14] the borylamides $Ni\{N(R)BMes_2\}_2$ (R = Ph or Mes),[15,16] the primary terphenyl amides $Ni\{N(H)Ar^{Me6}\}_2$,[17] $Ni\{N(H)Ar^{iPr4}\}_2$,[18] and $Ni\{N(H)Ar^{iPr6}\}_2$[17] ($Ar^{Me6} = C_6H_3$-2,6-(C_6H_2-2,4,6-Me_3)$_2$, $Ar^{iPr4} = C_6H_3$-2,6(C_6H_3-2,6-$^iPr_2$)$_2$, $Ar^{iPr6} = C_6H_3$-2,6(C_6H_2-2,4,6-$^iPr_3$)$_2$), and $Ni\{N(SiMe_3)Dipp\}_2$ (Dipp = C_6H_3-2,6-$^iPr_2$).[19,20] Computations indicated that the latter and its Fe and Co analogues are probably stabilized by attractive interligand dispersion forces.[21,22]

We showed recently[23] that the earlier reports on $Co\{N(SiMe_3)_2\}_2$[1,10] actually described its THF complex $Co\{N(SiMe_3)_2\}_2$(THF).[23,24] This prompted us to re-investigate the synthesis of the elusive $Ni\{N(SiMe_3)_2\}_2$ (**1**). We found that the addition of two equivalents of $Na\{N(SiMe_3)_2\}$ to a THF slurry of NiI_2 at 0 °C gave a red solution which upon workup gave a red oil (Scheme 1; see Supporting Information). Distillation yielded $Ni\{N(SiMe_3)_2\}_2$(THF) (**2**) instead of the earlier reported $Ni\{N(SiMe_3)_2\}_2$,[2] as a mobile red liquid. Storage at

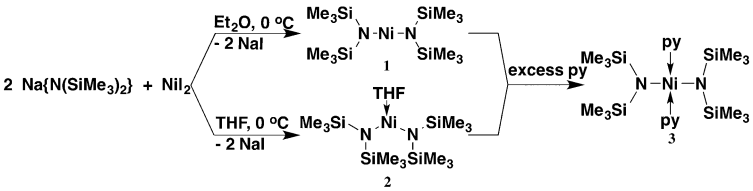

Scheme 1. Summary of the synthesis of $Ni\{N(SiMe_3)_2\}_2$ (**1**) and its THF and pyridine complexes **2** and **3**.

−18 °C gave green crystals of **2** suitable for X-ray diffraction. The THF-free $Ni\{N(SiMe_3)_2\}_2$ (**1**) was obtained using diethyl ether as a solvent. It distilled as a red vapor which condensed to give a yellow crystalline solid which has not yet proved amenable to X-ray crystallography. Crystals of **1** and **2** become black at room temperature and must be stored below −18 °C. ^{1}H NMR spectroscopy in C_7D_8 indicated that both **1** and **2** are paramagnetic and display a broad singlet at ca. 11 ppm due to the -$N(SiMe_3)_2$ protons. Complex **2** also features downfield THF proton signals which shift upfield at higher temperatures (Figure S5 in the Supporting Information), consistent with dissociation of THF, as also seen for its Mn and Co analogs.[23,25] Treatment of **1** or **2** with excess pyridine gave the diamagnetic bis(pyridine) complex *trans*-$Ni\{N(SiMe_3)_2\}_2(py)_2$ (**3**) as gold crystals. Complex **3** is stable as a crystalline solid or in pyridine solution at 25 °C, but dissociation of pyridine ligands in NMR solvents results in rapid decomposition.

For the structures of **2** and **3** (Figure 1), **2** has essentially trigonal planar geometry at Ni (Σ° Ni 359.86°) and it narrowly misses having a C_2 axis along the Ni–O bond, like its Fe and

[*] M. Faust, A. M. Bryan, Prof. M. M. Olmstead, Prof. P. P. Power
Department of Chemistry, University of California, Davis
One Shields Avenue, Davis, CA 95616 (USA)
E-mail: pppower@ucdavis.edu

A. Mansikkamäki, P. Vasko, Prof. H. M. Tuononen
Department of Chemistry, NanoScience Center
University of Jyväskylä
P.O. Box 35, FI-40014 Jyväskylä (Finland)
E-mail: heikki.m.tuononen@jyu.fi

Prof. F. Grandjean, Prof. G. J. Long
Department of Chemistry, Missouri University of Science and Technology, University of Missouri
Rolla, MO 65409-0010 (USA)

Supporting information for this article is available on the WWW under http://dx.doi.org/10.1002/anie.201505518.

 © 2015 Wiley-VCH Verlag GmbH & Co. KGaA, Weinheim

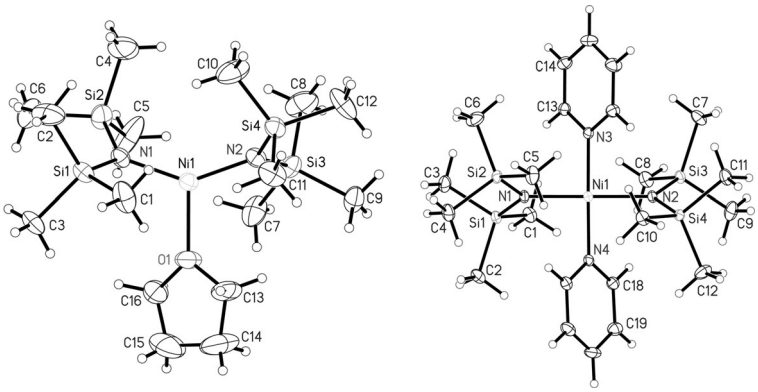

Figure 1. Thermal ellipsoid (50%) plots of $Ni\{N(SiMe_3)_2\}_2(THF)$ (**2**, left) and $Ni\{N(SiMe_3)_2\}_2(py)_2$ (**3**, right). Selected bond lengths (Å) and angles (°) for **2**: Ni1–N1 1.8646(2), Ni1–N2 1.8570(2), Ni1–O1 2.0143(2); N1-Ni1-N2 140.664(5), N1-Ni1-O1 109.42(19), N2-Ni1-O1 109.78(19); **3**: Ni1–N1 1.9394(4), Ni1–N2 1.9449(4), Ni1–N3 1.9305(4), Ni1–N4 1.9314(4); N1-Ni1-N2 179.2607(3), N3-Ni1-N4 179.0992(2).

Co analogs.[12,23,24] The Ni–N (1.8646(2) and 1.8570(2) Å) and Ni–O (2.0143(2) Å) bonds in **2** are shorter by 0.05 and 0.02 Å than the Co–N and Co–O bonds in its Co analog (Table S2). However, the Ni–N bond lengths are similar to those in $Ni\{N(Mes)BMes_2\}_2$ (avg. 1.866 Å).[15,16] The bis(pyridine) complex **3** has nearly ideal square planar coordination at Ni with interligand angles near 90°. The $Ni–N(SiMe_3)_2$ bonds (1.9394(4) and 1.9449(4) Å) are longer than those in **2** by 0.08 Å, which is likely due to the higher coordination number and increased steric crowding in **3**. The Ni–N bonds are longer than those in $Ni\{N(Mes)BMes_2\}_2$, (avg. 1.866 Å),[16] $Ni\{N(SiMe_3)Dipp\}_2$ (1.8029(9) Å),[21] $\{Ni(NPh_2)_2\}_2$ (avg. 1.828 Å for terminal Ni–N bonds),[14] and $Ni\{N(H)Ar\}_2$ (Ar = terphenyl) (avg. 1.821 Å).[17,18]

Originally, Bürger and Wannagat reported that blood red "$Ni\{N(SiMe_3)_2\}_2$" (probably $Ni\{N(SiMe_3)_2\}_2(THF)$) turned black after a short time at room temperature.[2] We also found that **1** and **2** became black within 30 min at 25 °C, but had greater stability as hydrocarbon solutions, whose red colors persist for 2–3 days at 25 °C. A sample of **1** in toluene decomposed over 4–5 weeks during which time the red solution became black and precipitated black crystals that were shown to be $[Ni\{N(SiMe_3)_2\}]_4$ (**4**) by X-ray crystallography. ^1H NMR spectroscopy of **2** in C_6D_6 indicated that decomposition to **4** yielded a second product which is $HN(SiMe_3)_2$ based on the observed singlet at ca. 0.1 ppm (Figure S7, Supporting Information). Compound **4** can also be synthesized from $LiN(SiMe_3)_2$ and $NiCl_2(DME)$ in Et_2O.[25] Workup of the dark amber solution afforded black crystals of **4** suitable for X-ray crystallography.

The structure of **4** (Figure 2) has four Ni^I ions in an approximate square plane and bridged by four $-N(SiMe_3)_2$ ligands. A C_2 axis bisects the N1 and N3 atoms, to give two crystallographically unique Ni1 and Ni2 sites on adjacent edges of the Ni_4 square. The N-Ni-N units deviate from linearity such that the Ni nuclei are displaced toward each other with Ni···Ni distances of 2.4328(4) and 2.4347(5) Å (cf. sum of single bond covalent radii for two Ni atoms = 2.20 Å).[27] The Ni···Ni distances in **4** are ca. 0.25 Å shorter than the Cu···Cu separations in $[Cu\{N(SiMe_3)_2\}]_4$,[2,25,28] 2.6770(7) and 2.6937(7) Å. Consistent with its bridging character, the average Ni–N bond length in **4** (1.916 Å) is longer than those in two-coordinate Ni^{II} amides (1.803(9)–1.885(4) Å)[15,18–20] and in the three-coordinate Ni^I amides $(Ph_3P)_2NiN(SiMe_3)_2$ (1.88(1) Å),[29] $[\{CHN(Dipp)\}_2C]NiN(SiMe_3)_2$ (1.865(2) Å),[30] and $(^tBu_2PCH_2CH_2P^tBu_2)Ni\{N(H)Dipp\}$ (1.882(2) Å).[31]

Magnetic studies of **4** yielded a χT versus T plot (Figure S14, Supporting Information) indicative of antiferromagnetic exchange between Ni^I centers. Since the coordination of the four nickels is essentially the same, the magnetic data were fit with the Hamiltonian $H = -2J\ (S_1S_2 + S_2S_3 + S_3S_4 + S_4S_1)$, assuming a single exchange coupling constant, J, for the Ni^I–Ni^I exchange. The best fit

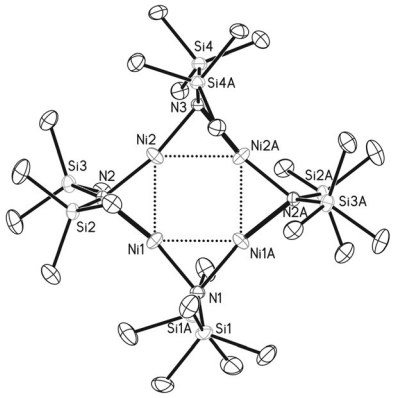

Figure 2. Thermal ellipsoid (50%) plot of $[Ni\{N(SiMe_3)_2\}]_4$ (**4**, without H atoms). Selected bond lengths (Å) and angles (°): Ni1–N1 1.9127(2), Ni1–N2 1.9151(2), Ni2–N2 1.9166(2), Ni2–N3 1.9189(2), Ni1···Ni2 2.4328(4), Ni1···Ni1A 2.4347(5); Ni1-N2-Ni2 78.77(1), N1-Ni1-N2 168.80(4), N2-Ni2-N3 168.90(4).

was obtained with $S_i = 1/2$ and $g = 2$ for the Ni ions, and yielded $J = -102(2)\ cm^{-1}$, a value typical for the exchange pathways involved. The singlet ground state of **4** is well reproduced by calculations at the CASSCF/NEVPT2 level of theory (see Supporting Information), but there are low-lying triplet and quintet states whose population at higher temperatures accounts for the μ_{eff} value of 2.70 μ_B measured for **4** at 300 K. The only other Ni^I species similar to **4** is $[Ni(NP^tBu_3)]_4$.[32] However, the two complexes differ structurally and magnetically. The N-Ni-N angles in $[Ni(NP^tBu_3)]_4$ are 180°, and the Ni_4N_4 core is folded along one of the N···N axes to yield a Ni···Ni separation of 2.375(3) Å (ca. 0.06 Å shorter than **4**). The magnetic moment of $[Ni(NP^tBu_3)]_4$ at 27 °C is 4.40 μ_B and indicates a larger contribution from higher spin states.

The ground state wave function for **4** is strongly multiconfigurational in character, as is evident from the CASSCF CI-vector or from the CASSCF natural orbital occupation numbers (Figure 3). Four electrons occupy four natural orbitals, roughly one each, that are composed of a set of nickel d-orbitals in four possible combinations. The natural

 © 2015 Wiley-VCH Verlag GmbH & Co. KGaA, Weinheim

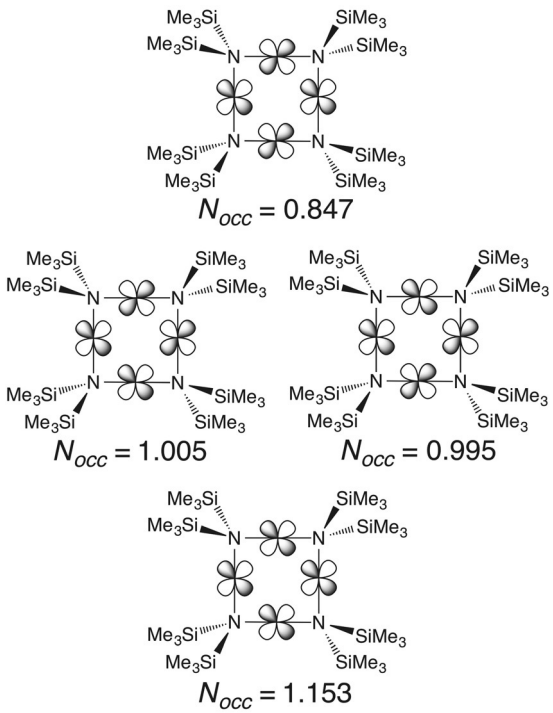

Figure 3. Most important natural orbitals and their occupation numbers from a CASSCF[4,4] calculation on **4**.

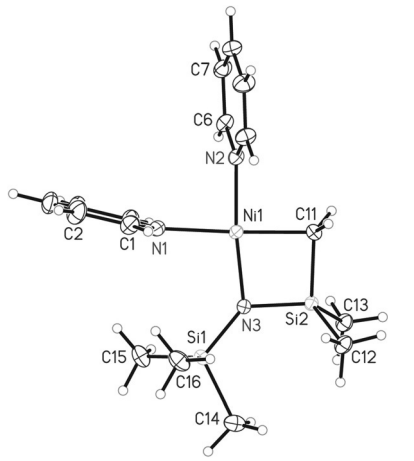

Figure 4. Thermal ellipsoid (50%) drawing of $Ni\{N(SiMe_3)(SiMe_2CH_2)\}(py)_2$ (**5**). Selected bond lengths (Å) and angles (°): Ni1–N1 1.9992(15), Ni1–N2 1.9119(15), Ni1–N3 1.9197(14), Ni1–C11 1.9707(17), Si2–C11 1.8329(17); N1-Ni1-N3 98.42(6); N2-Ni1-N3 87.51(6), N3-Ni1-C11 89.72(6), C11-Ni1-N1 84.41(6).

orbitals show both bonding and anti-bonding Ni···Ni character. However, since the occupancies of the fully bonding (1.153) and anti-bonding (0.847) combinations deviate significantly from 1, there remains some very weak metal···metal bonding character in **4**. More detailed magnetic and computational studies of **4** are in hand.

The experimental data clearly show that the stability of **1** is far lower than its Mn, Fe, or Co analogs. The decomposition of **1** into **4** involves cleavage of Ni–N bonds with reduction of Ni^{II} to Ni^{I}, the exact mechanism of which is unknown. The energetics of the decomposition process can, however, be evaluated at dispersion corrected DFT level (LC-ωPBE-D3/def-TZVP) by making the assumption that the formation of $HN(SiMe_3)_2$ involves hydrogen abstraction from the solvent (ether). The results show that homolytic cleavage of one of the Ni–N bonds in **1** has a high energetic penalty, and the formation of **4**, $HN(SiMe_3)_2$ and a diethyl ether radical is only barely exergonic, -2 kJ mol^{-1}. We note that the dispersion correction plays in this instance a major role by lowering the calculated reaction energy as much as 85 kJ mol^{-1}. In contrast, similar calculations for the Co analog of **1** show that the formation of a putative $[Co\{N(SiMe_3)_2\}]_4$ tetramer is endergonic by as much as 154 kJ mol^{-1} even with dispersion. It should be noted that the calculations do not take solvent effects into account nor is the fate of the ether radical modelled in any way. The predicted qualitative trend should, however, be unaffected by these, and indicates significant differences in the stability of the Ni^{I} and Co^{I} products. Additional support for the large energy difference comes from the $M^{I/II}$ oxidation potentials of the related amido M^{I} monoanions $[M\{N(SiMe_3)_2Dipp\}_2]^-$ (-0.152 and -1.082 V for Co and Ni, respectively),[33] which indicate that with amido ligands the process $Ni^{II} \rightarrow Ni^{I}$ is more favored than $Co^{II} \rightarrow Co^{I}$.

Indirect evidence for homolytic Ni–N dissociation comes from the reaction of $Na\{N(SiMe_3)_2\}$ and NiI_2 in pyridine which yielded an orange solution. Workup gave two crystalline products: orange blocks of $Ni\{N(SiMe_3)(SiMe_2CH_2)\}(py)_2$ (**5**) and gold needles of the aforementioned **3** in a ca. 3:1 ratio. In **5** (Figure 4), Ni is bound to two *cis*-oriented pyridines, an amido nitrogen, N3, and the carbon from a deprotonated Si2 methyl group. The C–H activation of methyl substituents in sterically crowded trimethylsilylamido transition metal complexes is well-known,[21,34–38] but **5** is apparently the first example for nickel. Complex **5** has distorted square planar geometry at Ni (Σ° Ni = 360.07°) and a lengthening of the Ni–py bond *trans* to the deprotonated methyl group, Ni1–N1 1.9992(15) Å (cf. 1.9197(14) and 1.9119(15) Å for Ni1–N3 and Ni1–N2). At 1.8329(17) Å, the Si2–C11 bond is shorter than the other Si–C bonds in **5** (avg. 1.883 Å). Another interesting feature of **5** is its slightly pyramidal geometry at N3 (Σ° N1 = 353.74°), whereas **2** and **3** have planar geometry at the amido nitrogens.

In conclusion, we have described the unstable Ni^{II} bis-silylamides $Ni\{N(SiMe_3)_2\}_2$ (**1**) and $Ni\{N(SiMe_3)_2\}_2(THF)$ (**2**) as well as the pyridine complex $Ni\{N(SiMe_3)_2\}_2(py)_2$ (**3**). We showed that **1** and **2** decompose to the tetrameric Ni^{I} amide $[Ni\{N(SiMe_3)_2\}]_4$ (**4**). The tetramer **4**, along with $Ni\{N\{N(SiMe_3)(SiMe_2CH_2)\}(py)_2$ (**5**), suggest that the decomposition of **1** and **2** formally occurs through homolytic fission of a Ni–N bond but the mechanistic details of this process are unkown. Computations indicate that the instability of **1** and **2** in comparison to their Mn, Fe, and Co analogs may be due to the greater tendency of Ni^{II} to be reduced as the energies of the d-electrons decrease across the 3d-series.[39] However, the quasi-stability of **1** and **2** in solution should permit their use as synthons, a use that is currently being investigated.

 © 2015 Wiley-VCH Verlag GmbH & Co. KGaA, Weinheim

Acknowledgements

We thank the National Science Foundation (Grant No. CHE-1263760) and the Academy of Finland (Grant Nos. 136929, 253907 and 272900) for funding. M.F., A.M.B., P.V. and A.M. thank the Livermore Graduate Scholar Program, NSF-GRFP (DGE-1148897), the Fulbright Center, and the Foundation for Research of Natural Resources in Finland for research fellowships and scholarships.

Keywords: dispersion effects · magnetism · nickel · silylamide · steric effects

How to cite: *Angew. Chem. Int. Ed.* **2015**, *54*, 12914–12917
Angew. Chem. **2015**, *127*, 13106–13109

[1] H. Bürger, U. Wannagat, *Monatsh. Chem.* **1963**, *94*, 1007–1012.
[2] H. Bürger, U. Wannagat, *Monatsh. Chem.* **1964**, *95*, 1099–1102.
[3] R. A. Andersen, K. Faegri, J. C. Green, A. Haaland, M. F. Lappert, W. P. Leung, K. Rypdal, *Inorg. Chem.* **1988**, *27*, 1782–1786.
[4] H. J. Gosink, H. W. Roesky, H. G. Schmidt, M. Noltemeyer, E. Irmer, R. Herbst-Irmer, *Organometallics* **1994**, *13*, 3420–3426.
[5] R. Anwander, *Chem. Mater.* **2001**, *13*, 4419–4438.
[6] E. Dumestre, B. Chaudret, C. Amiens, P. Renard, P. Fejes, *Science* **2004**, *303*, 821–823.
[7] B. A. Frazier, P. T. Wolczanski, E. B. Lobkovsky, T. R. Cundari, *J. Am. Chem. Soc.* **2009**, *131*, 3428–3429.
[8] J. Yang, T. D. Tilley, *Angew. Chem. Int. Ed.* **2010**, *49*, 10186–10188; *Angew. Chem.* **2010**, *122*, 10384–10386.
[9] T. Deschner, K. W. Tornroos, R. Anwander, *Inorg. Chem.* **2011**, *50*, 7217–7228.
[10] D. C. Bradley, K. J. Fisher, *J. Am. Chem. Soc.* **1971**, *93*, 2058–2059.
[11] D. C. Bradley, M. B. Hursthouse, K. M. A. Malik, R. Moseler, *Transition Met. Chem.* **1978**, *3*, 253–254.
[12] M. M. Olmstead, P. P. Power, S. C. Shoner, *Inorg. Chem.* **1991**, *30*, 2547–2551.
[13] P. P. Power, *Chemtracts* **1994**, *6*, 181–195.
[14] H. Hope, M. M. Olmstead, B. D. Murray, P. P. Power, *J. Am. Chem. Soc.* **1985**, *107*, 712–713.
[15] R. A. Bartlett, H. Chen, P. P. Power, *Angew. Chem. Int. Ed. Engl.* **1989**, *28*, 316–317; *Angew. Chem.* **1989**, *101*, 325–327.
[16] H. Chen, R. A. Bartlett, M. M. Olmstead, P. P. Power, S. C. Shoner, *J. Am. Chem. Soc.* **1990**, *112*, 1048–1055.
[17] A. M. Bryan, W. A. Merrill, W. M. Reiff, J. C. Fettinger, P. P. Power, *Inorg. Chem.* **2012**, *51*, 3366–3373.
[18] J. Li, H. Song, C. Cui, J.-P. Cheng, *Inorg. Chem.* **2008**, *47*, 3468–3470.
[19] M. I. Lipschutz, T. D. Tilley, *Chem. Commun.* **2012**, *48*, 7146–7148.
[20] P. P. Power, *Chem. Rev.* **2012**, *112*, 3482–3507.
[21] C.-Y. Lin, J.-D. Guo, J. C. Fettinger, S. Nagase, F. Grandjean, G. J. Long, N. F. Chilton, P. P. Power, *Inorg. Chem.* **2013**, *52*, 13584–13593.
[22] V. A. Parsegian, *Van der Waals Forces*, Cambridge University Press, Cambridge, **2006**.
[23] A. M. Bryan, G. J. Long, F. Grandjean, P. P. Power, *Inorg. Chem.* **2013**, *52*, 12152–12160.
[24] A. Eichhöfer, Y. Lan, V. Mereacre, T. Bodenstein, F. Weigand, *Inorg. Chem.* **2014**, *53*, 1962–1974.
[25] P. G. Eller, D. C. Bradley, M. B. Hursthouse, D. W. Meek, *Coord. Chem. Rev.* **1977**, *24*, 1–95.
[26] L. G. L. Ward, *Inorg. Synth.* **1972**, *13*, 154–164.
[27] P. Pyykkö, M. Atsumi, *Chem. Eur. J.* **2009**, *15*, 186–197.
[28] A. M. James, R. K. Laxman, F. R. Fronczek, A. W. Maverick, *Inorg. Chem.* **1998**, *37*, 3785–3791.
[29] D. C. Bradley, M. B. Hursthouse, M. B. Smallwood, A. J. Welch, *J. Chem. Soc. Chem. Commun.* **1972**, 872–873.
[30] C. A. Laskowski, G. L. Hillhouse, *J. Am. Chem. Soc.* **2008**, *130*, 13846–13847.
[31] D. J. Mindiola, G. L. Hillhouse, *J. Am. Chem. Soc.* **2001**, *123*, 4623–4624.
[32] J. Camacho-Bunquin, M. J. Ferguson, J. M. Stryker, *J. Am. Chem. Soc.* **2013**, *135*, 5537–5540.
[33] C.-Y. Lin, J. C. Fettinger, F. Grandjean, G. J. Long, P. P. Power, *Inorg. Chem.* **2014**, *53*, 9400–9406.
[34] C. R. Bennett, D. C. Bradley, *J. Chem. Soc. Chem. Commun.* **1974**, 29–30.
[35] S. J. Simpson, R. A. Andersen, *Inorg. Chem.* **1981**, *20*, 3627–3629.
[36] R. P. Planalp, R. A. Andersen, A. Zalkin, *Organometallics* **1983**, *2*, 16–20.
[37] P. Berno, S. Gambarotta, *Organometallics* **1994**, *13*, 2569–2571.
[38] M. A. Putzer, J. Magull, H. Goesmann, B. Neumüller, K. Dehnicke, *Chem. Ber.* **1996**, *129*, 1401–1405.
[39] D. M. P. Mingos, *Essential Trends in Inorganic Chemistry*, OUP, Oxford, **1998**.
[40] CCDC 1401113, 1401114, 1401115, and 1401116 contains the supplementary crystallographic data for this paper. These data can be obtained free of charge from The Cambridge Crystallographic Data Centre via www.ccdc.cam.ac.uk/data_request/cif.

Received: June 15, 2015
Revised: July 30, 2015
Published online: September 2, 2015

 © 2015 Wiley-VCH Verlag GmbH & Co. KGaA, Weinheim